Published in final edited form as:
J Neurosci. 2010 February 17; 30(7): 2600–2610. doi:10.1523/JNEUROSCI.3744-09.2010.

Cilia organize ependymal planar polarity

Zaman Mirzadeh[1,2], **Young-Goo Han**[1,2], **Mario Soriano-Navarro**[3], **Jose Manuel García-Verdugo**[3], and **Arturo Alvarez-Buylla**[1,2]

[1]Department of Neurosurgery, University of California, San Francisco, San Francisco, CA 94143, USA

[2]Eli and Edythe Broad Center of Regeneration Medicine and Stem Cell Research, University of California San Francisco, San Francisco, CA 94143, USA

[3]Laboratorio de Morfología Celular, Unidad Mixta CIPF-UVEG, CIBERNED, Valencia 46012, Spain

Abstract

Multi-ciliated epithelial cells, called ependymal cells, line the ventricles in the adult brain. Most ependymal cells are born prenatally and are derived from radial glia. Ependymal cells have a remarkable planar polarization that determines orientation of ciliary beating and propulsion of cerebrospinal fluid (CSF). Disruption of ependymal ciliary beating, by injury or disease, results in aberrant CSF circulation and hydrocephalus, a common disorder of the central nervous system. Very little is known about the mechanisms guiding ependymal planar polarity and whether this organization is acquired during ependymal cell development or is already present in radial glia. Here we show that basal bodies in ependymal cells in the lateral ventricle walls of adult mice are polarized in two ways: i) rotational; angle of individual basal bodies with respect to their long axis and ii) translational; the position of basal bodies on the apical surface of the cell. Conditional ablation of motile cilia disrupted rotational orientation, but translational polarity was largely preserved. In contrast, translational polarity was dramatically affected when radial glial primary cilia were ablated earlier in development. Remarkably, radial glia in the embryo have a translational polarity that predicts the orientation of mature ependymal cells. These results suggest that ependymal planar cell polarity is a multi-step process initially organized by primary cilia in radial glia and then refined by motile cilia in ependymal cells.

Keywords

ependymal cell; radial glia; primary cilia; planar cell polarity; basal body; hydrocephalus

Introduction

Ependymal cells are multiciliated epithelial cells that line the walls of the ventricular system in the adult brain. These cells are polarized in the epithelial plane, and this planar polarity is essential for propelling cerebrospinal fluid (CSF), which helps redistribute and dilute local concentrations of toxins and metabolites (Del Bigio, 1995). Early in neurodevelopment, the embryonic ventricles are lined by a germinal epithelium. This embryonic neuroepithelium has planar polarity that drives morphogenetic movements essential for neural tube closure (Colas and Schoenwolf, 2001; Wallingford, 2006). Later, radial glial cells within this epithelium contain both spatial and temporal patterning that determines cell fate and cell position in the

Corresponding Author: Arturo Alvarez-Buylla, PhD The Eli and Edythe Broad Center of Regeneration Medicine and Stem Cell Research 513 Parnassus Avenue, Room HSW-1201, Campus Box 0525 San Francisco, CA 94143-0525 Tel: (415) 514-2348 Fax: (415) 514-2346 abuylla@stemcell.ucsf.edu.

developing brain (Hebert and Fishell, 2008). A subpopulation of radial glia transform into ependymal cells (Spassky et al., 2005). Yet, planar cell polarity within individual radial glial cells has not been described and the mechanism by which ependymal cells develop their unique polarity remains unknown.

Ependymal cells extend multiple motile (9+2) cilia from their apical surface into the ventricles (Bruni, 1998). Planar-polarized beating of these cilia generates directed CSF flow (Worthington and Cathcart, 1963; Ibanez-Tallon et al., 2004; Sawamoto et al., 2006) and helps maintain CSF homeostasis (Cathcart and Worthington, 1964) (Del Bigio, 1995). Recent evidence also suggests that ependymal-generated CSF flow establishes gradients of chemorepellents that guide the migration of young neurons in the adult mammalian subventricular zone (Sawamoto et al., 2006).

Disrupting ependymal ciliary beating results in an accumulation of CSF in the brain ventricles and is a pathogenic mechanism of hydrocephalus (Nakamura and Sato, 1993; Ibanez-Tallon et al., 2004), one of the most common anomalies of the central nervous system (Bruni et al., 1985). In addition to hydrocephalic mouse models where the genetic defect disrupts ciliary motility (Torikata et al., 1991; Ibanez-Tallon et al., 2004) or ciliogenesis (Chen et al., 1998; Sapiro et al., 2002; Davy and Robinson, 2003; Banizs et al., 2005), human patients with primary ciliary dyskinesia also develop hydrocephalus (Jabourian et al., 1986; al-Shroof et al., 2001; Ibanez-Tallon et al., 2002; Wessels et al., 2003; Afzelius, 2004). The planar polarized beating of ependymal cilia is therefore essential for normal brain function. However, very little is known about the mechanism of planar cell polarity in ependymal cells.

Although there are functional assays for the planar polarity of ependymal cells, which measure the orientation of fluid flow above the surface of the epithelium (Ibanez-Tallon et al., 2004; Sawamoto et al., 2006), the cellular mechanism of this polarity is not known. We examined the basal bodies of ependymal cells by electron microscopy and immunofluorescence confocal microscopy. We found that two parameters of ependymal cell basal bodies, their rotational orientation and their translational position on the apical surface, correlated with the direction of fluid flow. Furthermore, by analyzing basal bodies in mutants that lack motile (9+2) cilia in ependymal cells or primary (9+0) cilia in their radial glial progenitors, we found that these two basal body parameters were differentially regulated. Finally, we found that the position of primary cilia on the apical surface of a subpopulation of radial glia was already polarized prior to their transformation into ependymal cells. Our results suggest that the primary cilium and its basal body apparatus may orchestrate the planar polarized architecture of both radial glia and their progeny ependymal cells.

Materials and Methods

Animals

All experiments were performed on mice according to the guidelines put forth by the UCSF Laboratory Animal Care and Use Committee. Mouse strains included CD-1 wild-type mice, and *hGFAP::Cre*, *Nestin::Cre*, *Kif3a-flox*, and *IFT88-flox* mice that were bred to produce conditional loss of cilia mutant mice.

Wholemount dissection

After cervical dislocation, the brain was removed from the skull and wholemounts of the lateral ventricle walls were freshly dissected as described (Mirzadeh et al., 2008). Briefly, a ventriculotomy was performed on each hemisphere to expose the walls of the lateral ventricle from their anterior to posterior extent. The exposed walls were then immersed in 4% paraformaldehyde at 4°C overnight.

Ependymal flow movies

Wholemounts of the lateral (or medial) wall of the lateral ventricle were freshly dissected and placed in 37°C Leibovitz media under a fluorescent stereomicroscope. A glass micropipette filled with fluorescent microbeads (2 μm) attached to a micromanipulator was lowered onto the wholemount, where microbeads were deposited onto the ventricular surface. We recorded the flow of microbeads using a Retiga 2000R high speed digital camera plugged into OpenLab imaging software (Improvision), with an acquisition rate of 10 frames per second.

Immunostaining and Microscopy

Primary and secondary antibodies were incubated in PBS with 0.5% TX and 10% normal goat serum for 24 hours at 4°C. Primary antibodies: mouse anti-acetylated tubulin (1:1000, Sigma T6793), rabbit anti-γ-tubulin (1:1000, Sigma T5192), mouse anti-β-catenin (1:500, BD Transduction Labs 610153), rabbit anti-β-catenin (1:1000, Sigma C2206), rat anti-CD24 (1:500, BD Pharmingen 557436), and chicken anti-GFP (1:500, Aves Labs GFP-1020). Secondary antibodies: conjugated to Alexa Fluor dyes (goat or donkey polyclonal, 1:400, Molecular Probes). Confocal images were taken on a Leica SP5 using a 100x oil objective (NA 1.46). Transmission electron microscopy analysis was performed as described (Doetsch et al., 1997). For reconstruction of the apical surface and basal bodies of E1 cells, we cut ~200 serial ultrathin (0.05 um) sections that were placed on Formvar-coated single-slot grids, stained with lead citrate, and examined under a Jeol 100CX EM.

Quantification of basal body patch angle

We wrote a program in Metamorph imaging software (Molecular Devices) to draw a vector connecting the center of two sequentially traced profiles: the apical surface of the cell and the area covered by that cell's basal body patch. The angle of this vector was called the BB patch angle. To determine the similarity of BB patch angles within a given high power field, we calculated the deviation of each cell's BB patch angle from the median within the field, and this data was plotted as a histogram. Only ependymal cells that had their entire apical surface within the high power field were analyzed. High power fields were of the following sizes: 127 × 127 μm^2 (P30 wild-type analysis, Figures 2 and S2), 89 × 89 μm^2 (P30 ciliary mutants analysis and E16, E18, and P1 wild-type analysis, Figures 3, 5, 6, S10, and S11). For the analysis of *hGFAP::Cre;Kif3a*$^{fl/fl}$ mutants (n=5) and control littermates (n=5), we analyzed 6 non-overlapping high power fields, 3 fields posterior to the adhesion area, along the dorsal-ventral midline of the lateral wall (corresponding to Region PM), and 3 fields anterior to the adhesion area along the dorsal-ventral midline. However, since *Kif3a* mutants lack an adhesion point, likely due to hydrocephalus and expanded ventricles, we could not use this landmark as a reference in mutants. Instead, the anterior-posterior position of high power fields taken in controls was recorded relative to the anterior boundary of the wholemount (0.2-0.7 mm for the anterior region and 1.7 to 2.5 mm for the posterior region) and corresponding fields were imaged and analyzed in mutant wholemounts. For *Nestin::Cre;Kif3a*$^{fl/fl}$ mutants, we imaged 10 non-overlapping high power fields (5 anterior and 5 posterior) to better approximate the true distribution of BB patch angles. For analysis of radial glial planar polarity at E16, E18, and P1, we examined 3 high power fields from each lateral wall studied (1 field in the anterior-ventral corner of the wholemount and 2 fields from a more posterior-ventral position near the foramen of Monro).

Quantification of basal body rotational orientation

Alignment of basal body rotational orientation was determined in ependymal cells by reconstructing their apical surface and basal bodies in ~200 serial en-face ultrathin sections. For basal bodies in each reconstructed ependymal cell, a vector was drawn from the center of the basal body barrel to the vertex of its basal foot and the angle of this vector was determined

using Metamorph software. We then calculated the deviation of each basal foot angle from the median basal foot angle within a cell and plotted deviation histograms similar to that for BB patch angles.

Results

Functional assays for ependymal planar polarity

We used fluorescent beads (2.0 μm diameter) placed on live preparations of the lateral wall of the lateral ventricle to measure direction and speed of ependymal flow (Figure 1A **and** Movie S1). This flow was highly stereotyped in 10 mice analyzed. The beads moved at speeds that ranged between 0.5-2 mm/s (10 beads analyzed per wholemount from 4 mice). The pattern of ependymal flow was studied in the anterior horn. Beads flowed in two streams: 1) dorsal - strong initial flow from posterior to anterior and then dorsal to ventral and 2) posterior - dorsal to ventral flow. Ependymal flow in the anterior horn appeared to be organized around the adhesion area and directed towards the foramen of Monro. These observations are consistent with previous studies (Sawamoto et al., 2006) in which India ink was used to visualize ependymal flow. We chose three regions around the adhesion area (depicted by red squares in Figure 1A) for the analysis shown in Figure 2 and Figure S2. The movement of fluorescent beads on the ventricular surface provided a dynamic assay for ependymal planar polarity and suggested how individual ependymal cells must be oriented in specific regions of this wall. The orientation of ependymal cells was confirmed by direct visualization of ciliary beating in region AD (Movie S2). The ciliary beating cycle consisted of two distinct bending forms that revealed this orientation, similar to what has been described for other multiciliated epithelia (Sanderson et al., 1990). These results demonstrated the stereotyped orientation of ependymal cells in specific regions of the ventricular wall and raised the question of the cellular properties that determine this exquisite planar polarity.

Cellular indicators of ependymal planar polarity

The basal foot, an electron-dense conical structure attached laterally to the basal body barrel, bestows rotational asymmetry to the basal body (Figure 1B). This is a useful indicator of the basal body's rotational orientation, which dictates the direction of fluid flow (Tamm et al., 1975; Marshall and Kintner, 2008). We examined, by electron microscopy (EM), basal foot orientation on the basal bodies of ependymal cells lining the lateral wall of the lateral ventricle. Ultrathin sections were cut in the plane parallel to the ventricular surface. Figure 1C shows two adjacent ependymal cells in region AD, where flow was directed in the anteroventral direction. The orientation of the image in Figure 1C and all subsequent images in this study correspond to the orientation of the lateral wall wholemount shown in Figure 1A. Figure 1D and 1E are higher power images of the boxed regions in Figure 1C, showing that basal feet of basal bodies in adjacent cells were well aligned (blue arrows indicate direction of basal foot). Additional examples are shown in Figure S1. Like other multiciliated epithelia (Boisvieux-Ulrich et al., 1985; Satir and Dirksen, 1985; Mitchell et al., 2007), the direction of the basal foot was aligned with the direction of fluid flow. The basal foot is therefore a reliable anatomical indicator of ependymal planar polarity.

Surprisingly, our EM analysis suggested that the position of the basal bodies themselves was polarized to one side of the ependymal cell apical surface. This corresponded to the side towards which the basal feet were directed (Figure 1C). Planar polarity of basal body position on the apical surface has not been reported in other multiciliated epithelia (Satir and Christensen, 2007). To investigate this planar organization, we immunostained wholemounts of the lateral wall of the lateral ventricle for γ-tubulin, which labels basal bodies, and β-catenin, an adherens junction component that delineates the apical cell surface (Mirzadeh et al., 2008)(Figures 2A, B). Ependymal cell basal bodies were clustered into a well-circumscribed patch (32-73 basal

bodies per patch, mean: 49) that accounted for 16±5% (range: 4-35%) of the total apical surface of ependymal cells. This enabled us to quantify the planar polarized position of the basal body patch relative to the apical surface. For this analysis, we wrote a program in Metamorph (Molecular Devices) that drew a vector from the center of the cell's apical surface to the center of the basal body patch (Figures 2C, D). The vector's angle was taken as a measure of the polarized position of the basal body patch on the apical surface. We will refer to this vector angle as the basal body (BB) patch angle. For each high power field (127 × 127 um^2), we calculated the deviation from the median BB patch angle of each cell's BB patch angle. This data was plotted on a histogram (Figures 2E, F). Clustering around 0° on this histogram would represent well-aligned BB patch angles (little deviation between cells). Our data from high power fields in regions AD and AV (175 cells analyzed in AD, 155 cells analyzed in AV from n=4 mice) indicated that BB patch angles were highly oriented in the ependymal layer. 87% of cells in region AD and 88% of cells in region AV had BB patch angles within 45° of the median. The median BB patch angles in these regions (averaged from n=4 mice, depicted by red arrows in Figures 2C, D) were correlated with the direction of CSF flow. Similar results were obtained for three other regions in the ventricular system (Figure S2), including region PM of the lateral wall of the lateral ventricle (region PM shown in Figure 1), region AV of the medial wall of the lateral ventricle (medial wall region AV shown in Figure S3), and a dorsal region of the 3rd ventricle wall. In addition, we confirmed the polarized position of BB patches by staining for ciliary bundles on the ventricular wall surface with antibodies for acetylated-tubulin, which labels the ciliary axoneme (Figure S4). These results showed that basal body patches were positioned on the “downstream” side of the ependymal cells’ apical surfaces, with respect to the direction of CSF flow.

Motile cilia are not essential for BB patch position but are required for BB rotational orientation

The “downstream” position of basal body patches on the apical surface of ependymal cells suggested that this anatomical planar polarity might be secondary to the mechanical force exerted by beating cilia on their basal body apparatus. In this scenario, the position of basal body patches is not an independent indicator of structural polarity within the cell, but rather a consequence of functionally polarized beating of cilia. To test this possibility, we conditionally ablated ependymal cilia by crossing mice expressing Cre under the human glial fibrillary acidic protein promoter (*hGFAP::Cre*) with mice carrying conditional *Kif3a* alleles (*Kif3a*$^{fl/fl}$). *Kif3a* encodes a subunit of the kinesin-2 motor that is essential for ciliogenesis (Kozminski et al., 1995). Cre expression in *hGFAP::Cre* mice begins in forebrain radial glia at E13.5 (Malatesta et al., 2003), and because ependymal cells are derived from radial glia (Spassky et al., 2005), this results in widespread recombination in the adult ependyma (Zhuo et al., 2001).

To determine when cilia are lost in *hGFAP::Cre;Kif3a*$^{fl/fl}$ mutants, we performed wholemount co-staining for acetylated-tubulin and γ-tubulin at P2, an age when radial glial transformation into ependymal cells has begun in the lateral ventricles (Spassky et al., 2005). This revealed that mutant ependymal cells lacked cilia associated with their multiple basal bodies (Figure S5F, arrowheads), but that radial glial cells had a primary cilium associated with a single basal body at their apical surface (Figures S5B, F). These results suggested that *hGFAP::Cre;Kif3a*$^{fl/fl}$ mutants lose cilia during the transformation from a radial glial cell with a primary cilium into an ependymal cell with multiple motile cilia. Consistently, ependymal cells in adult *hGFAP::Cre;Kif3a*$^{fl/fl}$ mutants lacked cilia (Figures 3A-D). As a consequence, these mutants had hydrocephalus (Figure S6).

Remarkably, the organization of basal body patches on the apical surface of ependymal cells lacking cilia was largely preserved (Figures 3E-H). To quantify this organization, we analyzed

6 non-overlapping high power fields (89×89 um^2) from each of 5 mutants (790 cells analyzed) and 5 control littermates (624 cells analyzed) at P30 (corresponding high power fields were analyzed in mutants and controls). In the absence of the ciliary axoneme, basal bodies in mutant ependymal cells were maintained in tightly clustered patches, accounting for 19%±6% of the total apical surface area, similar to controls at 22%±7% (Figures 3E, F). Moreover, the BB patch angles in the mutant ependyma were highly oriented, with only a small increased deviation from the median compared to controls (Figures 3G-I). Figure 3I is a histogram, similar to histograms of BB patch angles in Figure 2, showing the distribution of BB patch angles around the median in mutant and control ependyma. Although mutant BB patch angles were more widely distributed around the median than in controls (curve fit test, $p<0.0001$), they were still highly clustered around the median. In the mutant, 75% cells had BB patch angles within 45° of the median, while in controls it was 90% cells. In addition, we compared the displacement of the BB patch from the center of the apical surface using the magnitude of the BB patch vector. To control for different sizes and shapes of apical surfaces, the magnitude of the vector was normalized by dividing by the length of the line drawn from the center of the apical surface, in the direction of the vector, to the cell perimeter (normalization method illustrated in Figure S7). The BB patch displacement was therefore represented as a ratio of the displacement along this line. As shown in Figure 3J, there was no difference in BB patch displacement between mutant and control ependyma (curve fit test, $p=0.9839$). This data suggested that motile cilia are not required for the planar polarization of basal body patches on the apical surface of ependymal cells, but they may have a role in optimizing this polarization. Therefore, the BB patch position was an independent indicator of structural planar polarity within ependymal cells, not reliant on functional planar polarity of beating cilia.

We next tested whether motile cilia were required for alignment of rotational orientation of basal bodies using EM of en-face ultrathin sections to evaluate the basal feet in mutant and control ependyma (Figures 4A-D). For basal bodies in each ependymal cell analyzed, a vector was drawn from the center of the basal body barrel to the vertex of its basal foot and the angle of this vector was determined using Metamorph software. We then calculated the deviation of each basal foot angle from the median basal foot angle within a cell. This data was plotted on a histogram, similar to that for BB patch angles (Figure 4E). Rotational orientation of basal bodies was highly aligned in control animals, with 97% basal feet within 45° of the median (n=3 mice, 330 basal bodies in 65 cells analyzed). However, in mutants, there was a dramatic reduction in this alignment, with only 54% within 45° of the median (n=3 mice, 750 basal bodies in 92 cells). This effect ($p<0.0001$) on the alignment of basal body rotational orientation, as compared to BB patch position, suggested that while motile cilia are not essential for translation positioning of basal bodies, they are required for proper rotational orientation. More generally, this showed that the translational position and rotational orientation of basal bodies are affected differently by ependymal cilia.

To verify that the misalignment of basal body rotational orientation in *hGFAP::Cre;Kif3a*$^{fl/fl}$ mutants was due to a defect in ciliogenesis, and not another potential function of Kif3a, we crossed *hGFAP::Cre* mice to mice carrying a conditional allele of *Ift88* (Haycraft et al., 2007). *Ift88* encodes intraflagellar transport homolog 88, another protein essential for ciliogenesis (Murcia et al., 2000). *hGFAP::Cre;Ift88*$^{fl/fl}$ mutants were hydrocephalic and lacked cilia in ependymal cells (data not shown). Consistent with the above observations, only 56% basal feet were within 45° of the median in *hGFAP::Cre;Ift88*$^{fl/fl}$ mice (n=2 mice, 569 basal bodies in 84 cells) compared with 99% in controls (n=2 mice, 271 basal bodies in 36 cells) (Figure S8). This confirmed that misalignment of basal body rotational orientation was due to defective ciliogenesis.

Radial glia exhibit basal body planar polarity before transformation into ependymal cells

The above results suggested that translational planar polarity of ependymal cell basal bodies might be established before ependymal cell differentiation occurs and before their extension of motile cilia. We therefore investigated for evidence of planar cell polarity on the apical surface of radial glia during late embryogenesis and perinatally, before their transformation into ependymal cells. We immunostained the lateral ventricular walls of E16, E18, and P1 wild-type mice for β-catenin, to demarcate cell borders, and γ-tubulin, to visualize the primary cilia basal bodies (Figure 5). The lateral ventricular walls at these ages are covered by densely packed, small apical surfaces of radial glial cells (Tramontin et al., 2003), identified by the presence of a single basal body associated with a primary cilium. A subset of these cells is undergoing transformation into ependymal cells (Spassky et al., 2005). As previously described, we observed that ependymal transformation occurs in a medial to lateral and posterior to anterior gradient (Figure S9). We also observed that radial glial apical surfaces were much smaller in anterior regions of the lateral wall than in posterior regions (compare Figure S10A to S10B and Figure S11A to S11B). At successively older ages from E16 to P5, radial glial apical surfaces in more anterior regions expanded, prior to the multiplication of the number of basal bodies at these apical surfaces. In addition, using γ-tubulin staining, we observed dense punctate deposits likely corresponding to deuterosomes (structure used to build multiple basal bodies (Spassky et al., 2005)) in some radial glia with expanded apical surfaces (deuterosomes indicated by arrow in P1 image in Figure 5). These γ-tubulin deposits were never observed in radial glia with apical surfaces measuring less than 25 um^2. This suggested that expansion of the apical surface was a feature of a radial glial cell undergoing ependymal transformation. Note that type B1 cells, the ventricle-contacting adult neural stem cells, maintain small apical surfaces postnatally (average 24 um^2) (Mirzadeh et al., 2008).

Remarkably, as early as E16, a subset of radial glia exhibited planar polarity in the position of the single basal body on the apical ending. We quantified this polarization with the same method used to analyze ependymal cells. This polarity became incrementally more refined across the population of radial glia between E16 and P1 (Figure 5): at E16, 43% radial glia had BB angles within 45° of the median (n=3 mice, 3197 cells), which increased to 51% at E18 (n=3 mice, 1727 cells), and 61% at P1 (n=3 mice, 2834 cells). Basal bodies in neighboring radial glia were displaced to the same side of the apical surface, which interestingly corresponded to the “downstream” side where ependymal cells will later in development concentrate their motile cilia. This was true for radial cells at different stages of transformation into ependymal cells, including radial glia with a small apical surface, those with larger apical surfaces, and those containing deuterosome-like structures (Figures 5, S10, and S11). This suggested that well in advance of the formation of multiciliated ependymal cells, radial glia have already developed planar polarity that is predictive of the future patterns of ventricular flow propelled by ependymal cells.

We also performed several subgroup analyses at P1. Figures S10A-C show that radial glia were equally well oriented whether in anterior or more posterior regions. The regions analyzed are indicated in Figure S9: 1) in the posterior region, or “transformation zone” (arrowhead in Figure S9) some ependymal differentiation had already begun while 2) more anteriorly (arrow in Figure S9), no ependymal cells were observed and radial glia were densely packed with small apical surfaces. This suggested that at P1, the developmental stage of individual cells was not an essential determinant of polarity. Furthermore, we directly tested whether acquisition of planar polarity was a feature of transforming radial glia, identified by their expanded apical surface, or whether cells with small apical surfaces also had polarized basal body position. As shown in Figure S10D, cells with apical surfaces measuring less than 25 um^2 also had well oriented basal body angles. There was not a statistically significant difference in the distribution

of BB angles between cells with apical surfaces measuring less than or more than 25 um^2. This suggested that radial glia themselves, prior to ependymal transformation, have planar polarity.

Primary cilia in radial glia are essential for subsequent BB patch position in ependymal cells

Recent evidence suggests that primary cilia are important regulators of planar cell polarity (Ross et al., 2005; Park et al., 2006; Jones et al., 2008). Our results showed that radial glia exhibited planar polarity in the position of their primary cilium and its associated basal body, which were predictive of the polarized position of BB patches in their progeny ependymal cells. To test whether radial glial primary cilia are required for ependymal planar polarity, we crossed *Kif3a*$^{fl/fl}$ mice with *Nestin::Cre* mice that express Cre under the *Nestin* promoter, which is active in radial glia at E10.5 (Graus-Porta et al., 2001). We analyzed the ventricular walls of *Nestin::Cre;Kif3a*$^{fl/fl}$ mutants at P2 and found that in addition to an absence of motile cilia in ependymal cells, with very few exceptions primary cilia of radial glia were also absent (Figure S5D, H). These mutants allowed us to assess the role of radial glial primary cilia in ependymal planar polarity.

We analyzed *Nestin::Cre;Kif3a*$^{fl/fl}$ mutants and control littermates at P30 using a similar approach as used for *hGFAP::Cre;Kif3a*$^{fl/fl}$ animals. Although mutants lacked both radial glial primary cilia and ependymal cell motile cilia, ependymal cells in these mice differentiated, expanded their apical surfaces and developed tightly clustered patches of basal bodies, accounting for 15%±6% of the apical surface, compared with 16%±6% in controls (Figures 6A, B). Interestingly, BB patch angles in *Nestin::Cre;Kif3a*$^{fl/fl}$ mutants were poorly oriented (Figure 6E, curve fit test, $p<0.0001$), with only 49% cells within 45° of the median (total 395 cells from n=2 mutants), compared with 94% cells in controls (total 257 cells from n=2 control littermates). Moreover, when directly compared with *hGFAP::Cre;Kif3a*$^{fl/fl}$ mutants, the BB patch angle distribution for *Nestin::Cre;Kif3a*$^{fl/fl}$ mutants was significantly wider ($p<0.0001$). Note, however, that even *Nestin::Cre;Kif3a*$^{fl/fl}$ mutants have some residual polarization in their BB patch angles.

In addition to this quantitative difference in the BB patch angle distribution between *Nestin::Cre;Kif3a*$^{fl/fl}$ and *hGFAP::Cre;Kif3a*$^{fl/fl}$ mice, we found a qualitative difference in the BB patch displacement. This parameter was not affected in *hGFAP::Cre;Kif3a*$^{fl/fl}$ mutants (Figure 3J). However, in *Nestin::Cre;Kif3a*$^{fl/fl}$ mutants, which also lack primary cilia in radial glia, there was a significant left shift of the BB patch displacement curve (Figure 6F, $p<0.0001$). This left shift corresponds to cells with more centrally positioned BB patches. This suggests that primary cilia, in addition to having a prominent role in aligning the BB patch angles, partially regulate the initial peripheral positioning of basal body patches. However, other factors must also be involved in this process because many ependymal cells in *Nestin::Cre;Kif3a*$^{fl/fl}$ mice do have peripherally placed BB patches. In sum, *Nestin::Cre;Kif3a*$^{fl/fl}$ mutants have a mixture of two different polarity phenotypes: some cells are “mis-polarized,” wherein they have peripherally positioned BB patches that are not aligned, while other cells are “non-polarized,” wherein their BB patch is centrally positioned. Ependymal basal body rotational orientation was not analyzed in *Nestin::Cre;Kif3a*$^{fl/fl}$ mice, which similar to *hGFAP::Cre;Kif3a*$^{fl/fl}$ mutants, also lack ependymal cilia and would be expected to have similarly disrupted rotational polarity.

Discussion

We have shown that, in addition to basal body rotational orientation indicated by the basal foot, the position of the basal body patch on the apical surface of ependymal cells is an anatomical correlate to their functional planar polarity, the oriented beating of their multiple cilia. The position of the basal body patch was measured with respect to the center of the cell's apical surface by a vector. The angle of this vector, which we call the basal body (BB) patch angle,

was highly consistent among neighboring cells in the epithelium and was correlated to the direction of fluid flow and ciliary beating throughout the adult ventricular system. Moreover, the orientation of BB patch angles was largely preserved in the absence of motile cilia, indicating that this was an independent indicator of ependymal cell polarity, not secondary to mechanical forces imposed by ciliary beating. While mutants lacking motile cilia had largely preserved basal body patch positioning, the rotational orientation of basal bodies within each patch was poorly aligned. Interestingly, basal body patch positioning in ependymal cells was more dramatically affected in mutants lacking primary cilia in radial glial progenitors. This suggested that radial glial primary cilia and/or their basal bodies have a prominent role in organizing ependymal planar polarity. Consistently, we present the first evidence of planar polarity in radial glial cells, evident in the position of single basal bodies on the apical surface of a subpopulation of radial glia. Figure 7 is a summary illustration of our results.

Motile vs. Primary cilia in basal body planar polarity

We found that in the absence of motile cilia in *hGFAP::Cre;Kif3a*$^{fl/fl}$ mutants, the position of the basal body patch on the apical surface of ependymal cells remained largely oriented. A more dramatic effect was observed on the rotational orientation of basal bodies, indicated by the direction of basal feet, which were poorly aligned in mutants lacking motile cilia. These data are consistent with recent findings in the multiciliated epithelium of the *Xenopus* larval skin, where the basal foot similarly points in the direction of the ciliary effective stroke and is used as a measure of anatomical planar polarity (Mitchell et al., 2007). In Xenopus larval skin, basal feet are initially roughly polarized in the posterior direction based on anterior-posterior tissue patterning. Subsequently, flow generated by ciliary beating refines the polarity of basal feet rotational orientation. These observations in Xenopus larvae are consistent with our observations suggesting that motile cilia are essential to orient the angle of basal feet. In this scenario, the absence of cilia and active flow in the *hGFAP::Cre;Kif3a*$^{fl/fl}$ mutant ependymal epithelium precluded the refinement phase and resulted in a failure to complete the polarization process. In addition, the absence of motile cilia might contribute to reduced ependymal planar polarity through other non cell-autonomous mechanisms. For example, *hGFAP::Cre;Kif3a*$^{fl/fl}$ mutants had hydrocephalus, which may distort the epithelium lining the ventricles and influence the polarity of ependymal cells. In addition, we cannot exclude the possibility that Kif3a may have functions in the assembly of basal bodies that are essential for its rotational orientation. This latter possibility is unlikely, given that in our own observations and that of others (Matsuura et al., 2002), elimination of Kif3a function does not affect basal body ultrastructural organization. Moreover, *hGFAP::Cre;Ift88*$^{fl/fl}$ mutants showed a remarkably similar rotational misalignment of basal bodies to that observed in *hGFAP::Cre;Kif3a*$^{fl/fl}$ mutants, further suggesting that the observed effects are due to defects in ciliogenesis.

Our analysis showed that radial glia in *hGFAP::Cre;Kif3a*$^{fl/fl}$ mice retain primary cilia in most of the ventricular epithelium. To study the role of primary cilia in young progenitors in this ventricular wall, we analyzed ependymal planar polarity in *Nestin::Cre;Kif3a*$^{fl/fl}$ mutants, which lack primary cilia in radial glial cells in addition to motile cilia in ependymal cells. Interestingly, basal body patch positioning was dramatically affected in these mutants, significantly more than in those lacking only motile cilia. In addition to greater variability in the orientation of basal body patches, ependymal cells in these mutants had significantly more centrally positioned basal body patches. This suggests that primary cilia have a role in the positioning of basal bodies on one side of the apical surface of ependymal cells. These data are intriguing in light of recent evidence that primary cilia and their associated basal bodies regulate planar polarity in other tissues. In both the mammalian cochlea and early neural tube, ciliary/basal body proteins regulate planar polarity (Ross et al., 2005). Disrupting Bardet-Biedl syndrome ciliary proteins results in misoriented stereociliary bundles on cochlear hair cells

and defects in neural tube closure due to failed convergent extension. In addition, these proteins genetically interact with Vangl2, a component of the conserved planar cell polarity (PCP) pathway, which regulates planar polarity in tissues from flies to mammals (Zallen, 2007). Interestingly, in *Xenopus*, components of the PCP pathway appear to regulate ciliogenesis (Park et al., 2006). In the multiciliated epithelium of *Xenopus* larval skin, PCP components Disheveled (Park et al., 2008) and Vangl2 and Frizzled (Mitchell et al., 2009) control rotational polarity of basal bodies. A recent study in the mammalian cochlea directly addressed the role of primary cilia in planar polarity. Conditional mutants unable to extend a primary cilium from the apical surface of cochlear hair cells fail to correctly orient the actin cytoskeleton or to extend planar polarized stereocilia (Jones et al., 2008). However, cilia-deficient cells do exhibit planar polarized membrane distribution of PCP pathway molecules. This study suggests that the primary cilium relays PCP signals from the cell membrane to the cytoskeleton. Interestingly, another recent study showed that *Ift88* mutant zebrafish embryos that lack all cilia have no apparent defects in PCP signaling (Huang and Schier, 2009). This study suggested that the basal body, not the ciliary axoneme, might be the key mediator of PCP signals. The present results suggest that the primary cilium and its associated basal body in radial glia play an important role in the planar organization of the cytoskeleton in advance of ependymal differentiation.

Radial glial planar polarity

We provide the first evidence of planar polarity in radial glia, indicated by the position of single basal bodies at the apical surface of these cells. Radial glia with both small and large apical surfaces, as well as cells in various stages of differentiation into ependymal cells, displayed this polarity, which was predictive of the polarity in their ependymal progeny. Polarized positioning of the basal body represents a powerful mechanism to organize cytoskeletal architecture. We propose two possible models describing how radial glia may acquire planar polarity: i) genetically; planar polarity information present in the early neural plate may be transmitted through successive generations of cells within the neuroepithelium to radial glia; ii) environmentally; radial glia, possibly through the primary cilium, may sense mechanical or chemical signals in the ventricle. At the earliest stages of neural development, neuroepithelial cells display a planar polarized behavior called convergent extension, which is essential for neural tube formation (Copp et al., 2003). It has been previously hypothesized that radial glia lining the embryonic brain ventricles contain positional information that is projected onto the developing cortex as a spatial code through the radial fiber (Rakic, 1988). The planar polarity of ependymal cells may be a read out of this spatial code; a translation of the ependymal cell's (or its radial glial progenitor's) position in the epithelial plane into a polarized orientation. Indeed, radial glial planar polarity may be indicative of more widespread, genetically determined planar polarity throughout the developing and mature brain. Alternatively, radial glia may acquire planar polarity information independently through signals detected by the primary cilium. Primary cilia are well known as mechanosensory transducers (Hildebrandt et al., 2009) and may be performing this function in radial glia. Late in embryonic development, before ependymal cell differentiation and cilia-driven CSF flow develop, radial glial primary cilia may function as detectors of the passive bulk flow generated by the production of CSF from the choroid plexus and its exit through the foramen of Monro. In this scenario, radial glia may interpret passive flow to orient in the plane of the epithelium, such that ependymal planar polarity develops through a positive feedback loop where flow begets flow.

Our study provides the first insight into organization of ependymal planar polarity, and more generally, has implications for developmental organization of the neuroepithelium. This work has clinical significance for human patients with hydrocephalus, one of the most common anomalies of the central nervous system, and for mechanisms guiding neuronal migration in the adult brain, which has recently been shown in the SVZ to depend on gradients of

chemorepellents established by ependymal flow (Sawamoto et al., 2006). Altogether, our data show that ependymal planar polarity is described by two parameters of the basal body that are dependent on primary and motile cilia in a multi-step process. Planar polarity of basal body translational position is present in radial glial progenitors and depends on the primary cilium, whereas planar polarity of basal body rotational orientation is dependent on motile cilia.

Supplementary Material

Refer to Web version on PubMed Central for supplementary material.

Acknowledgments

We thank P. McQuillen for use of Metamorph software, B. Yoder for *Ift88*$^{fl/fl}$ mice, R. Romero-Rodriguez for ultrathin sectioning, and J. Reiter and W. Marshall for discussion. Work supported by NIH grant HD-32116, the Sandler Family Supporting Foundation and The John Bowes Stem Cell Fund. Z.M. supported by the Carlos Baldoceda Foundation and UCSF Krevans Fellowship. A.A.-B. holds the Heather and Melanie Muss Endowed Chair.

References

Afzelius BA. Cilia-related diseases. J Pathol 2004;204:470–477. [PubMed: 15495266]

al-Shroof M, Karnik AM, Karnik AA, Longshore J, Sliman NA, Khan FA. Ciliary dyskinesia associated with hydrocephalus and mental retardation in a Jordanian family. Mayo Clin Proc 2001;76:1219–1224. [PubMed: 11761503]

Banizs B, Pike MM, Millican CL, Ferguson WB, Komlosi P, Sheetz J, Bell PD, Schwiebert EM, Yoder BK. Dysfunctional cilia lead to altered ependyma and choroid plexus function, and result in the formation of hydrocephalus. Development 2005;132:5329–5339. [PubMed: 16284123]

Boisvieux-Ulrich E, Laine MC, Sandoz D. The orientation of ciliary basal bodies in quail oviduct is related to the ciliary beating cycle commencement. Biol Cell 1985;55:147–150. [PubMed: 2937490]

Bruni JE. Ependymal Development, Proliferation, and Functions: A Review. MicroscResTech 1998;41:2–13.

Bruni JE, Del Bigio MR, Clattenburg RE. Ependyma: Normal and pathological. A review of the literature. Brain ResRev 1985;9:1–19.

Cathcart RS 3rd, Worthington WC Jr. Ciliary Movement in the Rat Cerebral Ventricles: Clearing Action and Directions of Currents. J Neuropathol Exp Neurol 1964;23:609–618. [PubMed: 14219100]

Chen J, Knowles HJ, Hebert JL, Hackett BP. Mutation of the mouse hepatocyte nuclear factor/forkhead homologue 4 gene results in an absence of cilia and random left-right asymmetry. J Clin Invest 1998;102:1077–1082. [PubMed: 9739041]

Colas JF, Schoenwolf GC. Towards a cellular and molecular understanding of neurulation. Dev Dyn 2001;221:117–145. [PubMed: 11376482]

Copp AJ, Greene ND, Murdoch JN. Dishevelled: linking convergent extension with neural tube closure. Trends Neurosci 2003;26:453–455. [PubMed: 12948650]

Davy BE, Robinson ML. Congenital hydrocephalus in hy3 mice is caused by a frameshift mutation in Hydin, a large novel gene. Hum Mol Genet 2003;12:1163–1170. [PubMed: 12719380]

Del Bigio MR. The ependyma: A protective barrier between brain and cerebrospinal fluid. Glia 1995;14:1–13. [PubMed: 7615341]

Doetsch F, Garcia-Verdugo JM, Alvarez-Buylla A. Cellular composition and three-dimensional organization of the subventricular germinal zone in the adult mammalian brain. JNeurosci 1997;17:5046–5061. [PubMed: 9185542]

Graus-Porta D, Blaess S, Senften M, Littlewood-Evans A, Damsky C, Huang Z, Orban P, Klein R, Schittny JC, Muller U. Beta1-class integrins regulate the development of laminae and folia in the cerebral and cerebellar cortex. Neuron 2001;31:367–379. [PubMed: 11516395]

Haycraft CJ, Zhang Q, Song B, Jackson WS, Detloff PJ, Serra R, Yoder BK. Intraflagellar transport is essential for endochondral bone formation. Development 2007;134:307–316. [PubMed: 17166921]

Hebert JM, Fishell G. The genetics of early telencephalon patterning: some assembly required. Nat Rev Neurosci. 2008

Hildebrandt F, Attanasio M, Otto E. Nephronophthisis: disease mechanisms of a ciliopathy. J Am Soc Nephrol 2009;20:23–35. [PubMed: 19118152]

Huang P, Schier AF. Dampened Hedgehog signaling but normal Wnt signaling in zebrafish without cilia. Development 2009;136:3089–3098. [PubMed: 19700616]

Ibanez-Tallon I, Gorokhova S, Heintz N. Loss of function of axonemal dynein Mdnah5 causes primary ciliary dyskinesia and hydrocephalus. Hum Mol Genet 2002;11:715–721. [PubMed: 11912187]

Ibanez-Tallon I, Pagenstecher A, Fliegauf M, Olbrich H, Kispert A, Ketelsen UP, North A, Heintz N, Omran H. Dysfunction of axonemal dynein heavy chain Mdnah5 inhibits ependymal flow and reveals a novel mechanism for hydrocephalus formation. Hum Mol Genet 2004;13:2133–2141. [PubMed: 15269178]

Jabourian Z, Lublin FD, Adler A, Gonzales C, Northrup B, Zwillenberg D. Hydrocephalus in Kartagener's syndrome. Ear Nose Throat J 1986;65:468–472. [PubMed: 3490960]

Jones C, Roper VC, Foucher I, Qian D, Banizs B, Petit C, Yoder BK, Chen P. Ciliary proteins link basal body polarization to planar cell polarity regulation. Nat Genet 2008;40:69–77. [PubMed: 18066062]

Kozminski KG, Beech PL, Rosenbaum JL. The Chlamydomonas kinesin-like protein FLA10 is involved in motility associated with the flagellar membrane. J Cell Biol 1995;131:1517–1527. [PubMed: 8522608]

Malatesta P, Hack MA, Hartfuss E, Kettenmann H, Klinkert W, Kirchhoff F, Gotz M. Neuronal or glial progeny: regional differences in radial glia fate. Neuron 2003;37:751–764. [PubMed: 12628166]

Marshall WF, Kintner C. Cilia orientation and the fluid mechanics of development. Curr Opin Cell Biol 2008;20:48–52. [PubMed: 18194854]

Matsuura K, Lefebvre PA, Kamiya R, Hirono M. Kinesin-II is not essential for mitosis and cell growth in Chlamydomonas. Cell Motil Cytoskeleton 2002;52:195–201. [PubMed: 12112134]

Mirzadeh Z, Merkle FT, Soriano-Navarro M, Garcia-Verdugo JM, Alvarez-Buylla A. Neural stem cells confer unique pinwheel architecture to the ventricular surface in neurogenic regions of the adult brain. Cell Stem Cell 2008;3:265–278. [PubMed: 18786414]

Mitchell B, Jacobs R, Li J, Chien S, Kintner C. A positive feedback mechanism governs the polarity and motion of motile cilia. Nature 2007;447:97–101. [PubMed: 17450123]

Mitchell B, Stubbs JL, Huisman F, Taborek P, Yu C, Kintner C. The PCP pathway instructs the planar orientation of ciliated cells in the Xenopus larval skin. Curr Biol 2009;19:924–929. [PubMed: 19427216]

Murcia NS, Richards WG, Yoder BK, Mucenski ML, Dunlap JR, Woychik RP. The Oak Ridge Polycystic Kidney (orpk) disease gene is required for left-right axis determination. Development 2000;127:2347–2355. [PubMed: 10804177]

Nakamura Y, Sato K. Role of disturbance of ependymal ciliary movement in development of hydrocephalus in rats. Childs Nerv Syst 1993;9:65–71. [PubMed: 8319234]

Park TJ, Haigo SL, Wallingford JB. Ciliogenesis defects in embryos lacking inturned or fuzzy function are associated with failure of planar cell polarity and Hedgehog signaling. Nat Genet 2006;38:303–311. [PubMed: 16493421]

Park TJ, Mitchell BJ, Abitua PB, Kintner C, Wallingford JB. Dishevelled controls apical docking and planar polarization of basal bodies in ciliated epithelial cells. Nat Genet 2008;40:871–879. [PubMed: 18552847]

Rakic P. Specification of cerebral cortical areas. Science 1988;241:170–176. [PubMed: 3291116]

Ross AJ, et al. Disruption of Bardet-Biedl syndrome ciliary proteins perturbs planar cell polarity in vertebrates. Nat Genet 2005;37:1135–1140. [PubMed: 16170314]

Sanderson, MJ.; Dirksen, ER.; Satir, P. Electron microscopy of respiratory tract cilia.. In: Schaufnagel, DE., editor. Electron Microscopy of the Lung. Marcel Dekker; New York: 1990. p. 47-69.

Sapiro R, Kostetskii I, Olds-Clarke P, Gerton GL, Radice GL, Strauss IJ. Male infertility, impaired sperm motility, and hydrocephalus in mice deficient in sperm-associated antigen 6. Mol Cell Biol 2002;22:6298–6305. [PubMed: 12167721]

Satir, P.; Dirksen, ER. Function-structure correlations in cilia from mammalian respiratory tract.. In: Fishman, AP.; Cherniak, NS.; Widdicombe, JG.; Gieger, SR., editors. Handbook of Physiology-The Respiratory System. American Physiological Society; Bethesda: 1985. p. 473-494.

Satir P, Christensen ST. Overview of structure and function of mammalian cilia. Annu Rev Physiol 2007;69:377–400. [PubMed: 17009929]

Sawamoto K, Wichterle H, Gonzalez-Perez O, Cholfin JA, Yamada M, Spassky N, Murcia NS, Garcia-Verdugo JM, Marin O, Rubenstein JL, Tessier-Lavigne M, Okano H, Alvarez-Buylla A. New neurons follow the flow of cerebrospinal fluid in the adult brain. Science 2006;311:629–632. [PubMed: 16410488]

Spassky N, Merkle FT, Flames N, Tramontin AD, Garcia-Verdugo JM, Alvarez-Buylla A. Adult ependymal cells are postmitotic and are derived from radial glial cells during embryogenesis. J Neurosci 2005;25:10–18. [PubMed: 15634762]

Tamm SL, Sonneborn TM, Dippell RV. The role of cortical orientation in the control of the direction of ciliary beat in Paramecium. J Cell Biol 1975;64:98–112. [PubMed: 45847]

Torikata C, Kijimoto C, Koto M. Ultrastructure of respiratory cilia of WIC-Hyd male rats. An animal model for human immotile cilia syndrome. Am J Pathol 1991;138:341–347. [PubMed: 1992761]

Tramontin AD, Garcia-Verdugo JM, Lim DA, Alvarez-Buylla A. Postnatal development of radial glia and the ventricular zone (VZ): a continuum of the neural stem cell compartment. Cereb Cortex 2003;13:580–587. [PubMed: 12764031]

Vigh B, Manzano e Silva MJ, Frank CL, Vincze C, Czirok SJ, Szabo A, Lukats A, Szel A. The system of cerebrospinal fluid-contacting neurons. Its supposed role in the nonsynaptic signal transmission of the brain. Histol Histopathol 2004;19:607–628. [PubMed: 15024719]

Wallingford JB. Planar cell polarity, ciliogenesis and neural tube defects. Hum Mol Genet 2006;15:R227–234. Spec No 2. [PubMed: 16987888]

Wessels MW, den Hollander NS, Willems PJ. Mild fetal cerebral ventriculomegaly as a prenatal sonographic marker for Kartagener syndrome. Prenat Diagn 2003;23:239–242. [PubMed: 12627427]

Worthington WC Jr. Cathcart RS 3rd. Ependymal cilia: distribution and activity in the adult human brain. Science 1963;139:221–222. [PubMed: 14001896]

Zallen JA. Planar polarity and tissue morphogenesis. Cell 2007;129:1051–1063. [PubMed: 17574020]

Zhuo L, Theis M, Alvarez-Maya I, Brenner M, Willecke K, Messing A. hGFAP-cre transgenic mice for manipulation of glial and neuronal function in vivo. Genesis 2001;31:85–94. [PubMed: 11668683]

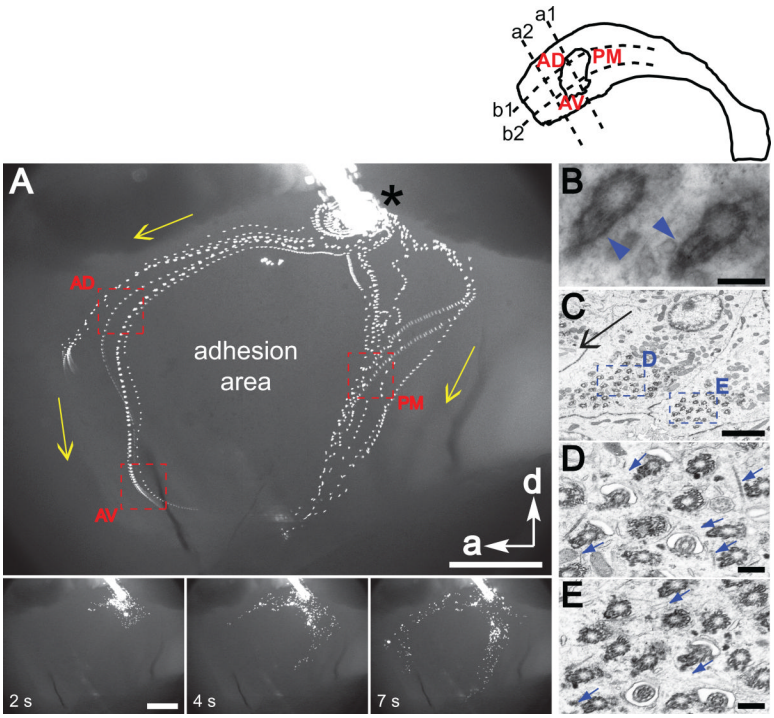

Figure 1. Functional planar polarity of the ependyma

Diagram at top right shows the lateral wall of the lateral ventricle divided by 4 lines into the regions analyzed: AD (anterior-dorsal), AV (anterior-ventral), and PM (posterior-middle). Line (a1) bisects the adhesion area into an anterior and posterior half. Line (a2) bisects the region between line (a1) and the anterior boundary of the wholemount. Line (b1) and (b2) run parallel along the anterior-posterior axis of the wholemount and divide the dorsal-ventral axis into 3 equal rows.

(A) Upper panel is from 89 consecutive frames of Movie S1 that were merged into a single picture. Fluorescent microbeads were deposited (*) on the surface of a wholemount of the lateral wall of the lateral ventricle. Oriented flow lines reveal planar polarized movement of beads above the ventricular wall surface driven by ependymal cilia. Each flow line represents sequential positions of a single bead. Yellow arrows indicate direction of flow. Anterior (a) and dorsal (d) directions are shown by white arrows. The adhesion area is where the medial and lateral walls are fused within the ventricular cavity; it is not covered by ependyma. Red boxes outline flow in regions AD, AV, and PM where cellular analyses in Figure 2 and S2 were performed. These regions are readily identified with respect to the adhesion area and their flow differs significantly: anteroventral in AD and PM, posteroventral in AV. Lower panels show individual frames of this movie. Scale bar = 0.5 mm.

(B) High power image of 2 ependymal cell basal bodies demonstrating the ultrastructure of the barrel and the basal foot (arrowheads) in cross-section. Scale bar = 200 nm.

(C) En-face electron micrograph near the apical surface of 2 adjacent ependymal cells in region AD. The orientation of this image and all subsequent images in this study correspond to the orientation of the wholemount in (A). Note clustering of basal bodies to one side of the apical surface in both cells. Higher power images of the basal bodies shown in (D) and (E) (boxed regions). Scale bar = 2 um.

(D, E) Some basal bodies in (C) were transected at the level of the basal foot. Orientation of the basal foot (blue arrows) is consistent within each cell and between cells and points in the direction of CSF flow (black arrow in (C)). Scale bar = 0.25 um.

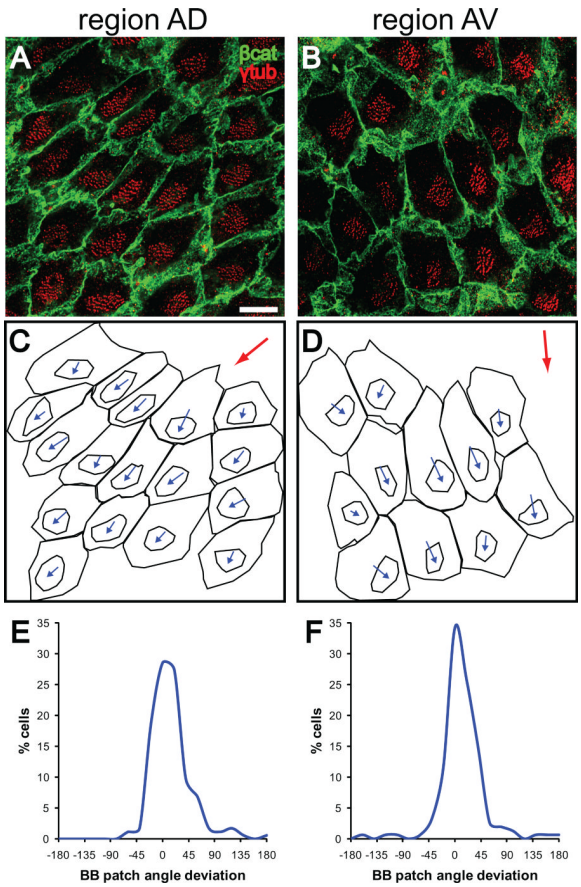

Figure 2. Basal body patch position is an anatomical indicator of ependymal planar polarity

(**A, B**) Confocal images from regions AD and AV (see Fig. 1A) of lateral wall wholemounts stained for β-catenin (green) and γ-tubulin (red). In both regions, the patch of basal bodies is located on the "downstream" side of the apical surface with respect to CSF flow (compare to flow in boxed regions in Fig. 1A). Scale bar = 10 um.

(**C, D**) Traces of the apical surfaces and basal body patches in (A, B). Basal body patch position was measured relative to the apical surface using a vector connecting the centers of these two traced regions for each cell. The angle of this vector was called the basal body (BB) patch angle. The red arrows indicate the direction of the median angle in the region.

(**E, F**) For each high power field analyzed, the difference between each cell's BB patch angle and the median BB patch angle in the field was calculated and this data was plotted on a histogram. The narrow distribution around 0° revealed that BB patch angles in these regions were highly oriented.

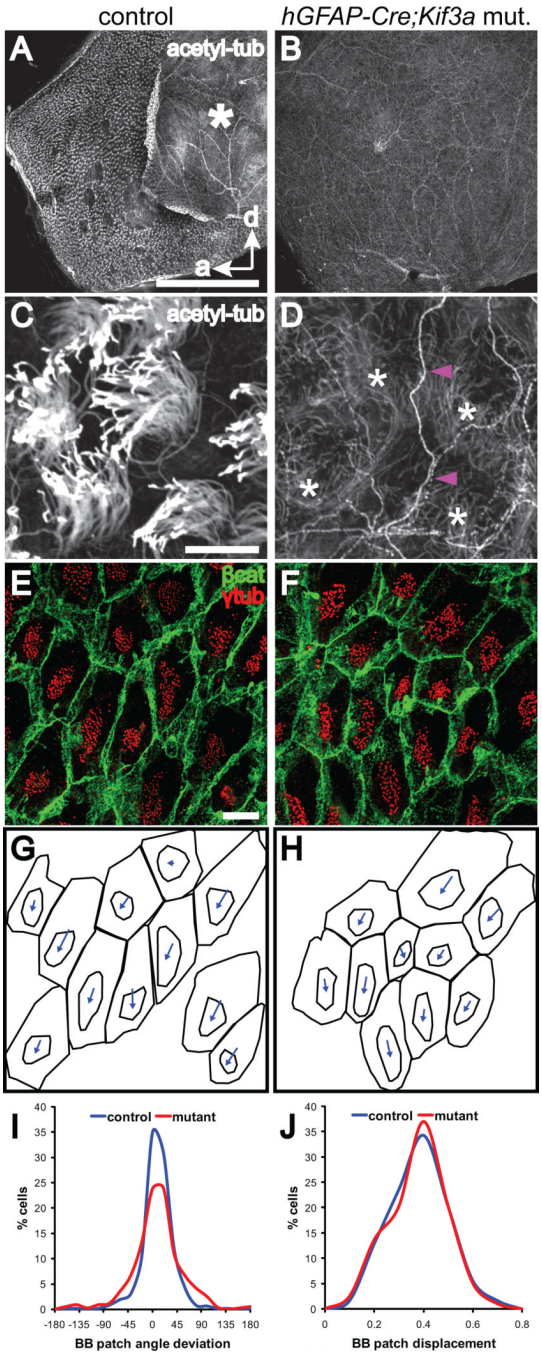

Figure 3. Planar polarity of basal body patches does not require motile (9+2) cilia

(A, B) Low power confocal images of lateral wall wholemounts from the LV of *hGFAP::Cre;Kif3a*$^{fl/fl}$ mutants and control littermates stained for acetylated-tubulin. Tufts of cilia, seen as small white puncta on the ependymal surface of controls at this magnification, are missing in mutants. Asterisk on the control wholemount indicates the adhesion area, which is not present in the mutant, likely due to hydrocephalus. Anterior (a) and dorsal (d) directions are indicated by arrows. Scale bar = 0.5 mm.

(C, D) High power confocal images from the wholemounts in (A, B) show that while microtubule-based cilia were absent on the apical surface of mutant ependymal cells, the microtubule network (*) within these cells was preserved. Note also that intraventricular axons

(magenta arrowheads), stained by acetylated-tubulin, were seen on the ventricular surface of both wholemounts, although more clearly on the cilia-deficient mutant ependyma. Intraventricular axons have been described previously (Vigh et al., 2004). Scale bar = 10 um.

(E, F) Confocal images of control and *hGFAP::Cre;Kif3a*$^{fl/fl}$ mutant lateral wall wholemounts stained for β-catenin (green) and γ-tubulin (red). Basal bodies in mutant ependymal cells were maintained in tightly clustered patches. The planar polarized position of these patches was also largely preserved in the absence of motile cilia. Scale bar = 10 um.

(G, H) Traces of the apical surfaces and basal body patches in (E, F), with vectors indicating the relative position of the BB patch.

(I) Histogram showing the distribution of BB patch angles around the median in control (blue) and mutant (red) ependyma. As indicated by the narrow distribution, the mutant ependyma had highly oriented BB patch angles (n=5 mutants (790 cells), 5 control littermates (624 cells); curve fit test, $p<0.0001$).

(J) Histogram showing the distribution of normalized BB patch displacement from center in control (blue) and mutant (red) ependyma (curve fit test, $p=0.9839$).

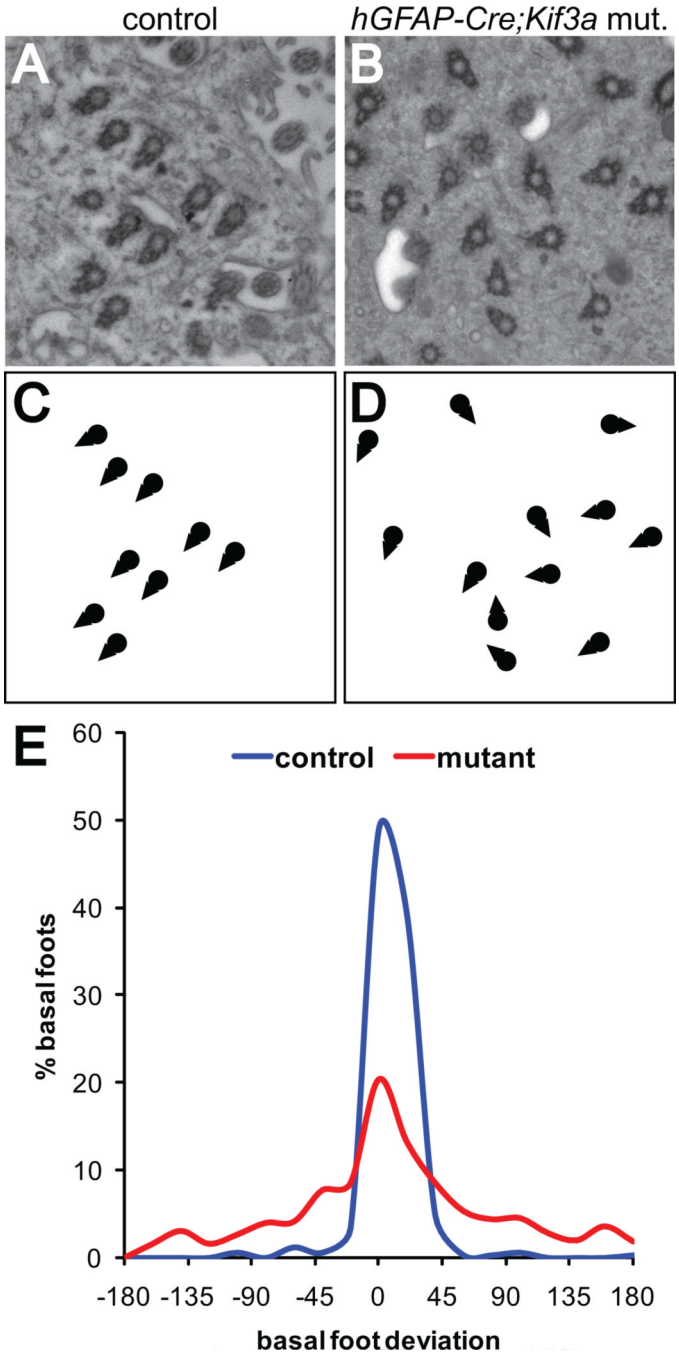

Figure 4. Alignment of basal body rotational orientation requires motile cilia

(A, B) En-face electron micrographs from the apical surface of control and *hGFAP::Cre;Kif3a*$^{fl/fl}$ mutant ependymal cells demonstrated the organization and rotational orientation of their basal bodies.

(C, D) Schematic drawings of the basal bodies shown in (A, B) illustrate the misalignment of basal body rotational orientation, indicated by triangle-shaped basal feet, in *hGFAP::Cre;Kif3a*$^{fl/fl}$ mutants.

(E) Histograms showing the distribution of basal foot angles around the median in control and *hGFAP::Cre;Kif3a*$^{fl/fl}$ mutant ependyma demonstrated that basal body rotational orientation

is significantly reduced in the absence of motile cilia ($p<0.0001$, n=3 control mice with 330 basal bodies in 65 cells analyzed, 3 mutant mice with 750 basal bodies in 92 cells).

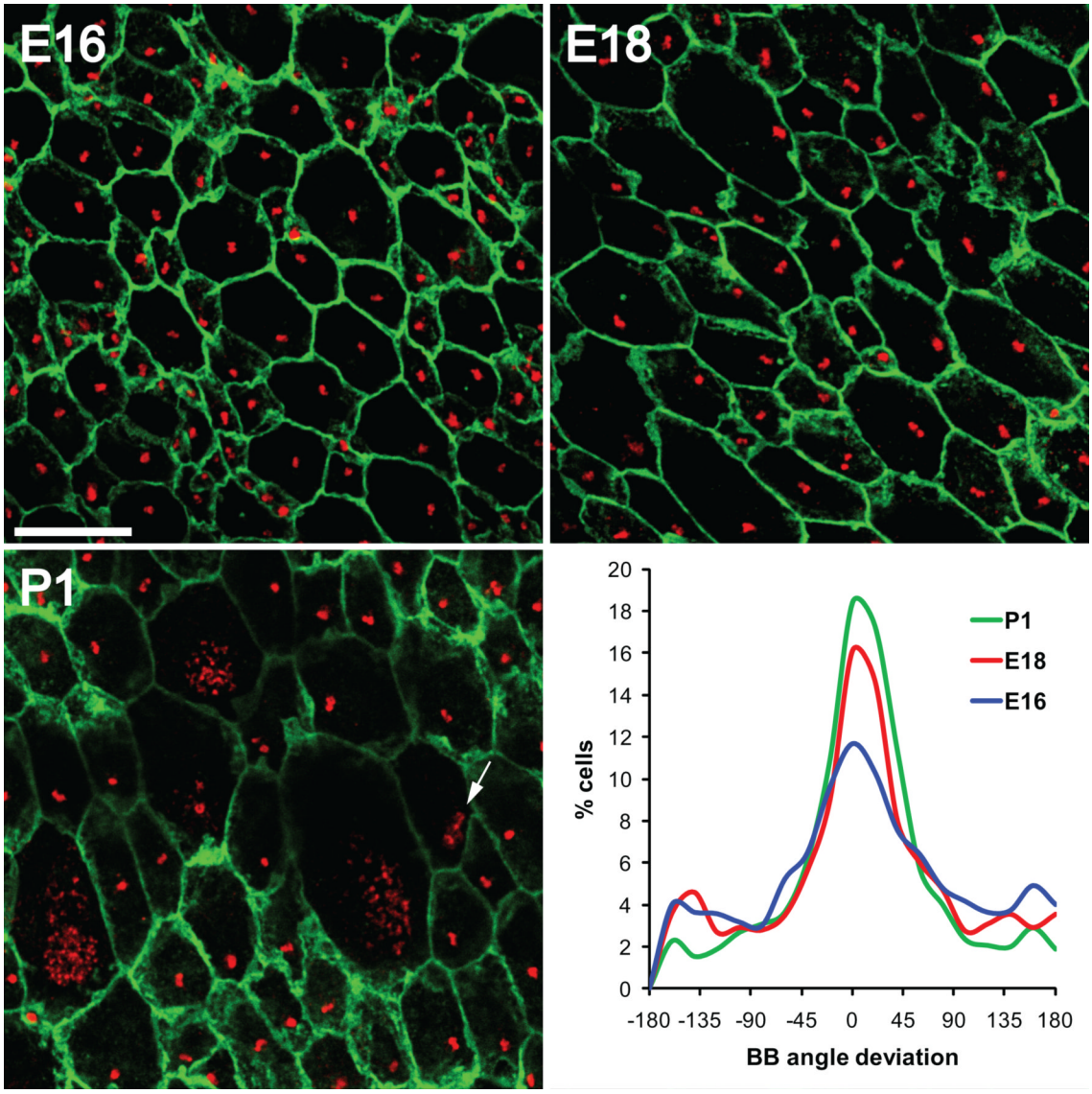

Figure 5. Planar polarity of basal body position in radial glia

Confocal images of lateral wall wholemounts from E16, E18, and P1 wild-type mice stained for β-catenin (green) and γ-tubulin (red). Images were taken from a mid-ventral region of the wholemount near the foramen of Monro (arrowhead in Figure S9). At successively older ages, radial glial apical surfaces expanded and by P1, some radial glia had already transformed into ependymal cells with multiple basal bodies. Note that some cells had dense punctate γ-tubulin staining likely corresponding to deuterosomes (arrow in P1 image). The histograms show that at successively older ages, an increasingly larger fraction of radial glia exhibited planar polarity of their single basal body. Neighboring cells had their basal body displaced to the ensuing "downstream" side of the cell with respect to CSF flow. Scale bar = 10 um.

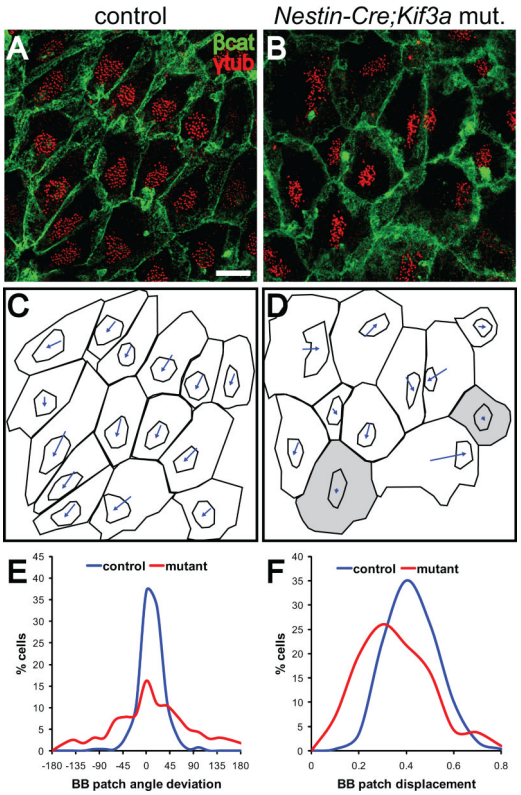

Figure 6. Planar polarity of ependymal basal body patches is disrupted by loss of primary cilia from radial glial progenitors

(A, B) Confocal images of control and *Nestin::Cre;Kif3a*$^{fl/fl}$ mutant lateral wall wholemounts stained for β-catenin (green) and γ-tubulin (red). Basal bodies in mutant ependymal cells were maintained in tightly clustered patches but the planar polarized position of these patches was less evident. Scale bar = 10 um.

(C, D) Traces of the apical surfaces and basal body patches in (A, B), with vectors indicating the relative position of the BB patch. Cells shaded in gray had BB patches that were not displaced from the cell center.

(E) Histogram showing the distribution of BB patch angles around the median in control (blue) and mutant (red) ependyma. Orientation of BB patch angles was dramatically disrupted in *Nestin::Cre;Kif3a*$^{fl/fl}$ mutants compared with controls (curve fit test, $p<0.0001$), also significantly more disrupted when compared directly with *hGFAP::Cre;Kif3a*$^{fl/fl}$ mutants ($p<0.0001$, see Figure 3I red curve).

(F) Histogram showing the distribution of normalized BB patch displacement from center in control (blue) and mutant (red) ependyma (curve fit test, $p<0.0001$). *Nestin::Cre;Kif3a*$^{fl/fl}$ mutants had ependymal cells with more centrally positioned BB patches.

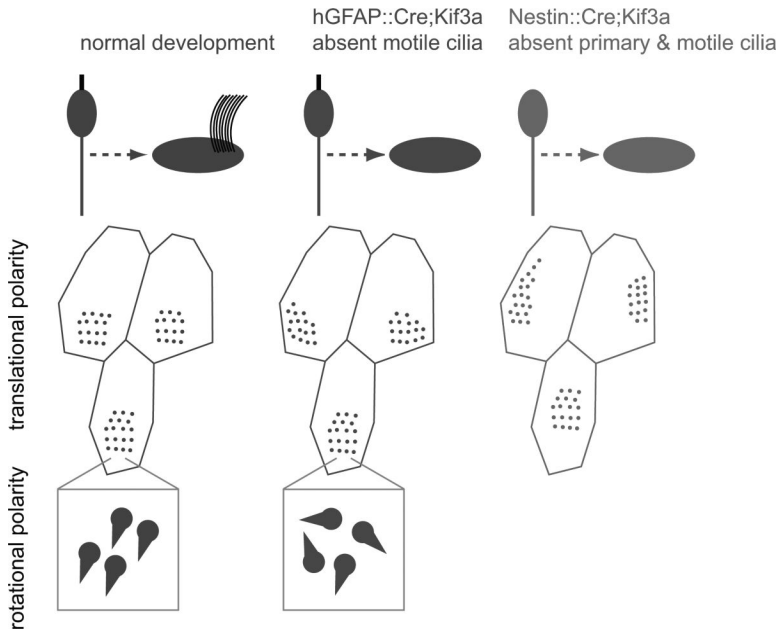

Figure 7.

Summary illustration of the roles of primary and motile cilia in ependymal planar polarity. Normal development of ependymal planar polarity is shown in the left column. Loss of motile cilia from ependymal cells (middle column) does not dramatically alter translational polarity of basal body patches but it disrupts their rotational polarity, while loss of both primary cilia from radial glial progenitors and motile cilia from ependymal cells (right column) dramatically disrupts translational polarity.